Available online at www.sciencedirect.com
ScienceDirect
Journal of the European Ceramic Society 29 (2009) 99–104
www.elsevier.com/locate/jeurceramsoc

The porosification of fired LTCC substrates by applying a wet chemical etching procedure

A. Bittner, U. Schmid *

Saarland University, Faculty of Natural Sciences and Technology II, D-66123 Saarbruecken, Germany

Received 7 December 2007; received in revised form 30 April 2008; accepted 9 May 2008
Available online 7 July 2008

Abstract

In this study, a novel process is presented to generate a defined and homogeneous degree of porosity in fired low temperature co-fired ceramics (LTCC) substrates. For this purpose, a phosphoric-based acid is used which is a standard wet chemical etchant in the MEMS and microelectronic industry for the patterning of aluminium-based conductors and strip lines. Varying the bath temperature between 90 and 130 °C within a time frame of up to 8 h, a maximum penetration depth of 40 μm is achieved. At short etch times up to 5 h, the porosification process is reaction controlled, while at longer exposure times, diffusion-related effects dominate verified by the determination of the corresponding activation energies. In combination with morphological investigations using scanning electron microscopy and micro-X-ray diffraction techniques, it is demonstrated that the anorthite-phase crystallizing during liquid sintering in the vicinity of the Al_2O_3 grains shows a high dissolvability in phosphoric acid and is very important to enable its penetration into the LTCC body. This surface-near process is very attractive for the realization of selected areas on conventional LTCC substrates having modified dielectric properties, especially for high frequency applications.

Keywords: Porosity; Dielectric properties; Glass ceramics; Substrates; Wet etching

1. Introduction

In recent years, low temperature co-fired ceramics (LTCC) have attracted much attention both as device and substrate structures. The possibility to implement vias with a low sheet resistance based on Au, Ag or Ag/Pd and the integration of passive electronic components (i.e. inductors, resistors and capacities) into the ceramic body, makes it possible to exploit the third dimension.[1,2] This enables the arrangement of electronic components in a compact way within a gas-proof body. Therefore, the components are well protected from environmental impacts when operated under harsh environmental conditions, such as high temperatures.[3] LTCC are commonly based on a glass–ceramic consisting of a glass matrix in which aluminium oxide particles with a typical diameter in the range of 2–3 μm are embedded as a filler material. For metallization purposes, the thick film printing technique is the standard technology used. Due to the low sintering temperatures with peak levels in the range of 850 °C the complete assembly of filled vias and printed structures is fired in one single step with the substrate. By the liquid-phase sintering process the soft sheets are densified to form the monolithic ceramic body.

On the device and system level, many novel and sophisticated approaches are reported in literature, such as the fabrication of miniaturized actuators,[4,5] different types of sensor elements for the determination of, i.e. force, gas concentration, mass flow or temperature[6–10] and even complete systems, especially for microfluidic applications.[11] A comprehensive overview is given in Refs.[12,13] In this context, reliability in respect to mechanical strength is an important issue, especially when the LTCC needs to fulfil not only the requirements of a functional, but also of a structural material subjected to high mechanical load.[14,15]

Besides these applications, LTCC is most favourably used as substrate for micromachined devices and systems operated at high frequencies typically ranging up to the microwave region. Although there are also other types of high-density, multilayer substrates available, based on organic laminates, further outstanding features of the LTCC for this field of application are the excellent thermal conductivity compared to organic mate-

* Corresponding author. Tel.: +49 681 302 4181; fax: +49 681 302 4669.
E-mail addresses: a.bittner@lmm.uni-saarland.de (A. Bittner), u.schmid@lmm.uni-saarland.de (U. Schmid).

0955-2219/$ – see front matter © 2008 Elsevier Ltd. All rights reserved.
doi:10.1016/j.jeurceramsoc.2008.05.030

rials and a coefficient of thermal expansion close to that of silicon.[13] Compared to a standard organic substrate reinforced with a glass–fibre-based component, such as FR-4 or RT/Duroid, the dielectric losses are low. In contrast, the relatively high permittivity of $\varepsilon_r = 7–8$ is disadvantageous for some applications, such as microwave antennas directly arranged on the LTCC surface. To avoid this drawback either a combination of LTCC with a local application of a low-k organic material[16] or the modification of the LTCC substrate itself is targeted. Beside the modification of the glass-matrix and the crystallization behaviour,[17,18] the generation of a defined porosity is the most commonly used approach to reduce the dielectric constant and the dielectric losses of materials.[19] In Refs.[20,21] mullite or ceramic-based bubbles are dispersed in the glass-matrix modifying the dielectric properties positively, but resulting in a poor topography, especially when aiming for the application of structures on the surface made by thin film technology. In addition, the use of hollow microspheres is proposed which causes problems when these break during casting and firing and hence, reproducible dielectric properties cannot be guaranteed.[22,23] Schuler et al. modulated the material properties by punching holes in the substrate.[24] The effective permittivity is determined by the volumetrically weighted median of the relative permittivity values associated with LTCC and air. In Ref.[25] the capacitive coupling between a strip line and ground plane is reduced by embedding air cavities below the conductor. Although in the latter two cases, a local modification of the dielectric properties is in principal possible, an additional ceramic layer has to be arranged above the perforated substrate to support the elements resulting in a fragile overall structure.

It is the objective of this paper to report a novel process to generate locally a defined porosity in LTCC in the fired state. Up to now, a maximum penetration depth for the porosification process of about 40 μm below the substrate surface has been achieved. Phosphoric-based acid is used which is a well-established chemical product used for the patterning of aluminium-based strip lines within the fabrication process of micromachined devices. The process and hence, the degree of porosification and the corresponding penetration depth, can be controlled at a given bath concentration very easily by monitoring the etch time and the temperature of the etchant. Both parameters have a high impact on the dominating etch regime (i.e. either reaction or diffusion-controlled). Applying techniques such as scanning electron microscopy (SEM), focused ion beam (FIB) and micro-X-ray diffraction (μ-XRD), the microstructure and the phase composition of the LTCC are investigated before and upon exposure to phosphoric acid.

2. Experimental details

To study the porosifiaction process, commercially available LTCC substrates (DP 951 AX) from DuPont are used. The blank sheets were laminated at a pressure of 20 MPa and fired at a peak temperature of 850 °C for 30 min in a batch furnace. Further details of the fabrication process can be found elsewhere.[26] After co-firing, a compound material is generated consisting of a glass matrix with different crystalline and chemical phases in which

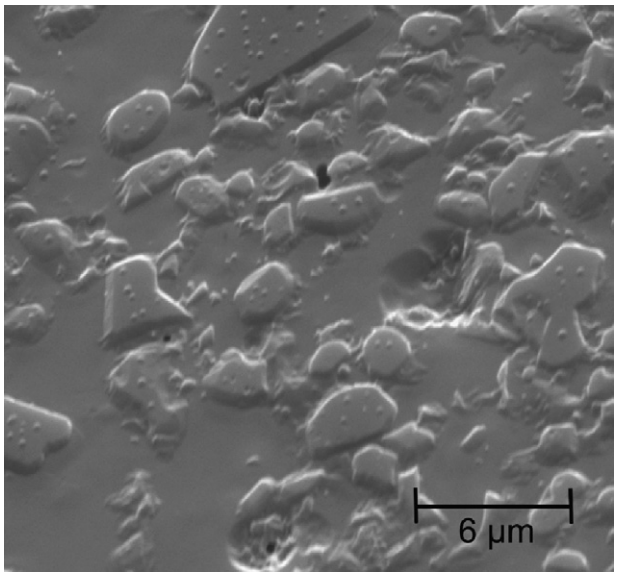

Fig. 1. SEM top view on a conventional LTCC (DP 951) substrate. To highlight the microstructure, the LTCC substrate is dry etched for several minutes applying an argon flux, thus removing the glass coverage from the surface.

Al_2O_3 particles with a typical size in the μm-range are implemented (see Fig. 1). Basically, the DuPont 951 LTCC consists after firing of corundum, anorthite and lead silicate glass.[27]

To chemically attack the LTCC substrates, phosphoric acid with a purity of 85 vol.% is used. The bath temperature is closed-loop controlled on a hotplate purchased from Heidolph Instruments and varied between 90 and 130 °C within time frames of 1–8 h. Finally, the samples were rinsed in deionized water and dried with purged air.

To measure the penetration depth of the porosification process, the specimens were embedded into a resin matrix (Demotec 30), grinded on a standard turntable from Struers for cross-sectional analyses and inspected via SEM technique (LEO 435VP). To investigate the micro-cavities and pores generated after wet chemical etching in more detail, an SEM in a "Dual Beam FIB—FEI Strata DB235" workstation was applied. In these cases, cross-sectioning was done by means of FIB technique.

For phase analyses μ-XRD measurements were performed using a diffractometer D8 GADDS from Huber Inc. The X-ray beam with a wavelength of 1.5418 Å corresponding to the Cu Kα-line is highly focused by an aperture with a spatial resolution of 50 μm and aligned on the sample by a video system with accuracy better than 100 μm. The 2D detector "HiStar" is from Bruker Inc.

3. Results and discussion

In Fig. 2, the porosification depth d_p in fired LTCC substrates as a function of time t at different bath temperature levels T_b of the phosphoric acid is shown. A minimum value for T_b of 90 °C is required to obtain in a time frame of about 1 h a detectable porosification depth of 30 nm. As expected, d_p increases when enlarging the duration for the etch attack at a given bath temper-

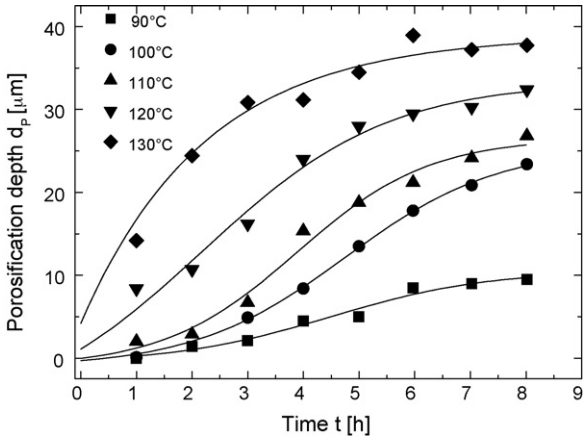

Fig. 2. Porosification depth d_p in LTCC (DP 951) as a function of time t at different bath temperatures of the phosphoric acid.

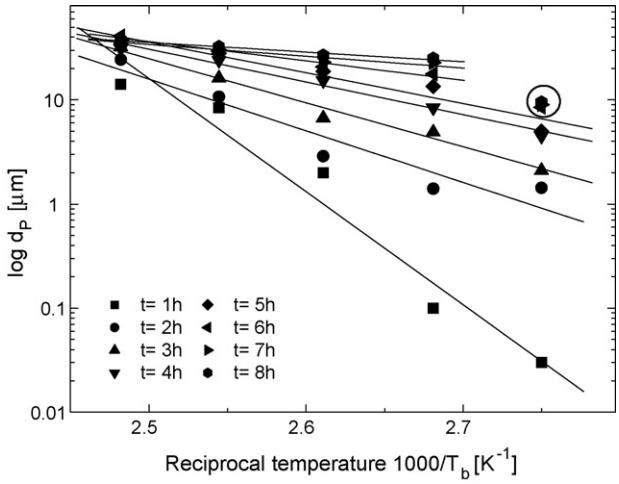

Fig. 3. Data of Fig. 2 arranged in an Arrhenius configuration.

ature. Increasing T_b has a similar impact on d_p while keeping the parameter t fixed. At the onset of the etch attack, d_p and hence, the porosification rate, is relatively low at $T_b = 90$ and 110 °C. In the range of 2–5 h, the corresponding values of d_p show a linear relationship with t before reaching a bath-temperature dependent saturation level. Excluding under these conditions a period of about 2 h at the beginning to activate the porosification process, the curves obey in principle a functional characteristic, well known, e.g. for the different growth regimes of silicon dioxide when subjected to a standard wet oxidation process of silicon substrates.[28] Therefore, it is assumed that up to a time frame of 5 h, the attack for the porosification process of LTCC is reaction-limited, while in the saturation regime, where the exchange of the etch solution from the surface through porous layer to the etch front in the LTCC body is dominant, it is diffusion-controlled. Increasing the bath temperature to 110 °C, the porosification process is activated above average resulting in an almost linear relationship between d_p and t from the very beginning of the process. In agreement to the lower bath temperatures investigated, the saturation regime establishes after a period of about 5 h resulting in a maximum porosification depth of about 40 µm. To verify these assumptions on the presence of the two major etch regimes, the activation energies are determined at fixed exposure times in an Arrhenius-type diagram from the corresponding slopes with a linear regression procedure (see Fig. 3).

Basically, the slope of the fitted lines decreases continuously with larger exposure time indicating reduced values for the corresponding activation energies.

In Fig. 4, the time-dependent evolution of E_a is shown with values ranging from about 0.2 eV at long etching periods up to 2.2 eV determined for a 1 h exposure. In principal, when a diffusion controlled reaction regime dominates in a wet etching process activation energies are about 0.2 eV. In contrast, higher activation energies indicate reaction limited dissolution rates.[29] In addition, the porosification depth as a function of reciprocal bath temperature obeys the Arrhenius law over the complete temperature range up to $t = 5$ h, as illustrated in Fig. 2. Above, the data points at $T_b = 90$ °C marked with a circle do not fit into this trend as at these low temperatures and at these low values for d_p, the etch process is still dominated by the reaction controlled regime in contrast to higher bath temperatures.

From the application-oriented point of view, this wet etching process provides a sufficient depth promising a substantial reduction of the dielectric properties, such as permittivity, for high frequency applications. In Fig. 5, a typical cross-sectional view on the surface-near porosification is shown used to extract the data presented in Fig. 2. Besides the determination of d_p, a constant value for this important porosification parameter is demonstrated on technical-relevant length scales, providing a homogeneous reduction in dielectric properties across a given area.

To investigate the nature of the porosification process and the corresponding microstructures in more detail, FIB technique in combination with SEM analyses were applied. For comparison purposes, Fig. 6a shows the topography of an "as manufactured" DP 951 LTCC substrate. The surface is highly undulated in the µm-range (i.e. $R_{max} \sim 1.7$ µm and $R_a \sim 0.4$ µm) due to the implemented Al_2O_3 particles and covered with the glass matrix due to the liquid-phase sintering process. After exposure to the phosphoric acid for 3 h at 90 °C, the glass matrix is locally

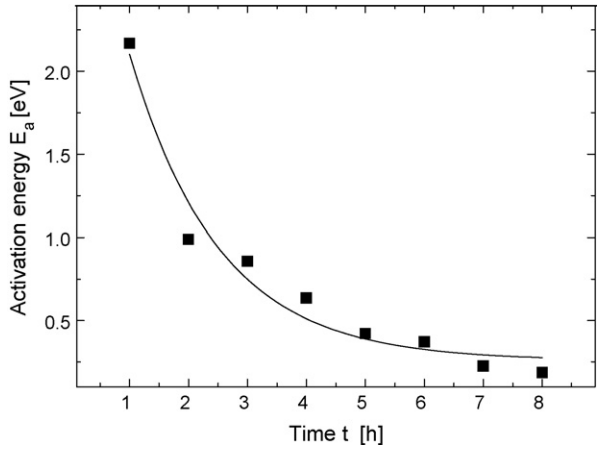

Fig. 4. Decreasing activation energies E_a while the porosification process. The inserted line serves as a guide to the eye.

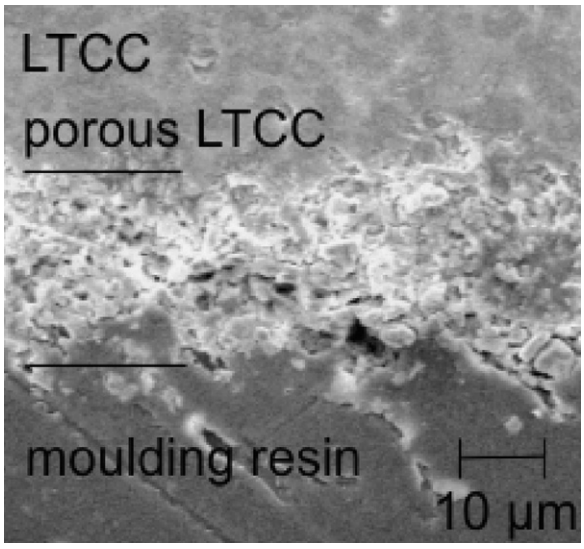

Fig. 5. Typical result when using a phosphoric acid at 110 °C for 5 h to generate a porous microstructure in LTCC.

attacked on the surface forming gaps and pores with dimensions well below 1 μm (see Fig. 6b). Increasing t to 8 h, the glassy top coverage is almost completely removed giving access to the Al_2O_3 particles located below (see Fig. 6c). After etching 8 h at 130 °C the glass-phase totally disappears (see Fig. 6d). Furthermore, the mean gap size is substantially increased indicating the penetration of the wet chemical into the body of the LTCC.

In Fig. 7a, a cross-sectional view of the porous layer is given after an etch attack at $T_b = 90$ °C for 8 h. As shown, the phosphoric acid penetrates via tiny gaps into the LTCC body. This is especially obvious in the area of the porosification front proceeding into the LTCC substrate where this portion of the glass matrix surrounding the Al_2O_3 particles is preferentially etched. Close to the surface, the formation of larger pores is indicated, as in this long etching regime, the Al_2O_3 grains are now selectively etched compared to the residual glass matrix. When increasing T_b, but decreasing t to 2 h, only the presence of sub-μm sized gaps and pores are detected supporting the findings on the porosification process drawn from Fig. 7b. Again, the results are similar to Fig. 7c when increasing on this high temperature level t to 8 h, besides a more pronounced pore formation and a larger penetration depth which cannot be fully exploited via FIB technique due to a depth range for characterization limited to about 20 μm. From these morphological investigations it can be concluded that the grain-near portion of the matrix is very important to enable the penetration of the phosphoric acid into the LTCC body.

For verification purposes, μ-XRD measurements are performed to determine any changes in phase composition before and upon exposure of LTCC to phosphoric acid. As illustrated in Fig. 8, a reduction of the anorthite concentration in the porous LTCC compared to the "as fired" state is demonstrated when analysing the (0 0 4) peak as the most dominant of the anorthite spectra. During liquid-phase sintering, the glass-phase near the alumina grains crystallizes to anorthite, which develops out of the glass matrix and aluminium whereas the latter originates from the alumina grains.[30] Due to the diffusion related crystallization of the anorthite this phase is generated with a thickness of about 500 nm enveloping the surface of the alumina grains. When taking the results presented in Figs. 6 and 7 into account, it is obvious that the anorthite-phase is etched predominantly at the beginning of the etch attack. This is due to a higher dissolvability of anorthite compared to alumina and the residual

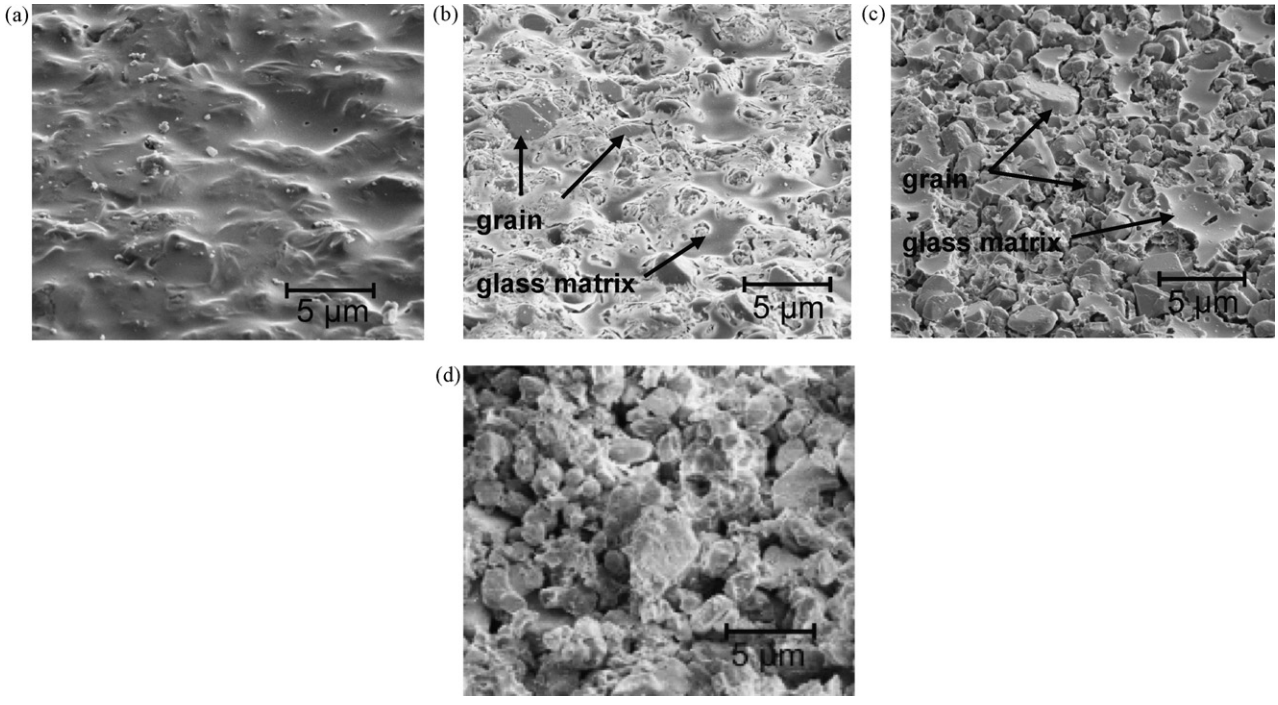

Fig. 6. Surface morphology of LTCC in different modifications: (a) "as manufactured", (b) after etching for 3 h at $T_b = 90$ °C, (c) after etching for 8 h at $T_b = 90$ °C, and (d) after etching for 8 h at $T_b = 130$ °C.

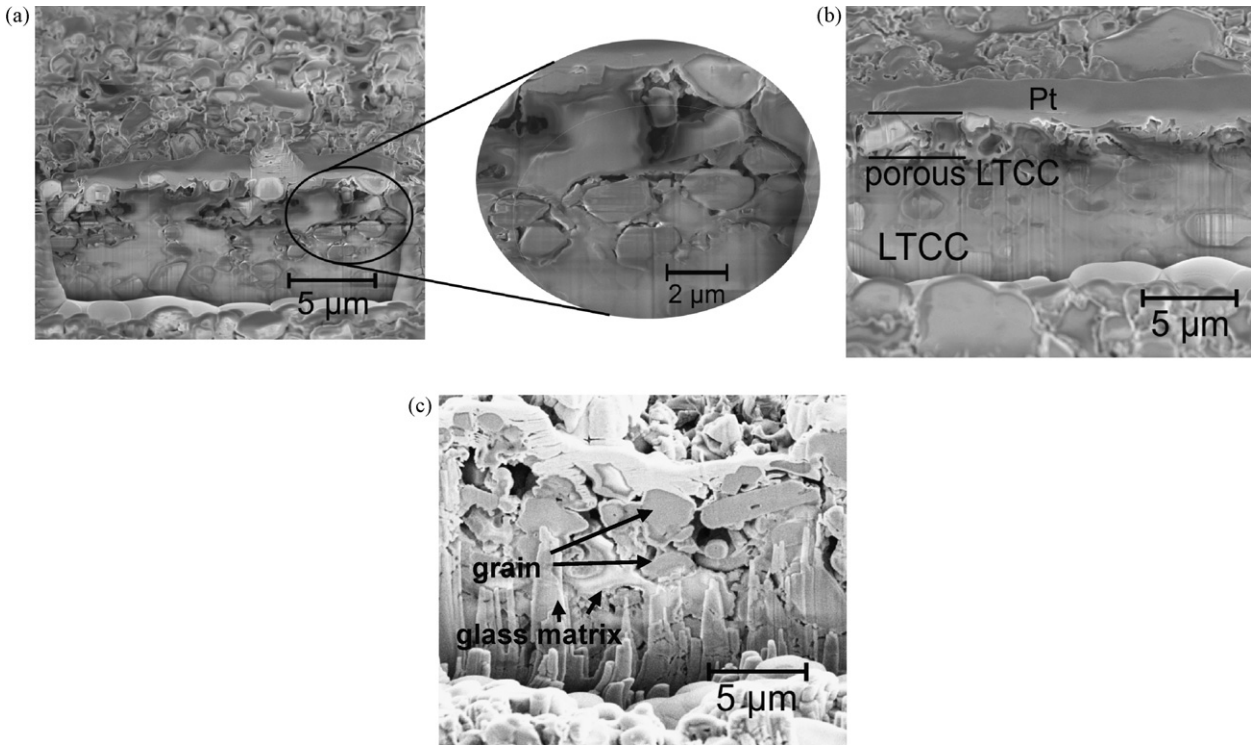

Fig. 7. Cross-sectional view on the microstructure of LTCC close to the surface. The glass-ceramic is etched in phosphoric acid for (a) 8 h at $T_b = 90\,^{\circ}C$, (b) 2 h at $T_b = 110\,^{\circ}C$ and for (c) 8 h at $T_b = 110\,^{\circ}C$. The platinum top layer is only applied to avoid any structural damage to the probe surface during FIB preparation procedure.

glass matrix and hence, is responsible for the penetration of the etchant. Basically, the dissolution of anorthite in acidic etchants is according to the following reaction[31]:

$$CaAl_2Si_2O_8 + 8H^+ \rightarrow Ca^{+2} + 2Al^{+3} + 2SiO_2(aq) + 4H_2O.$$

Typical values for the corresponding activation energies of silicates in aqueous solutions are in the range of 0.6–0.8 meV[32] fitting well to the data determined for the porosification process in this work (see Fig. 4).

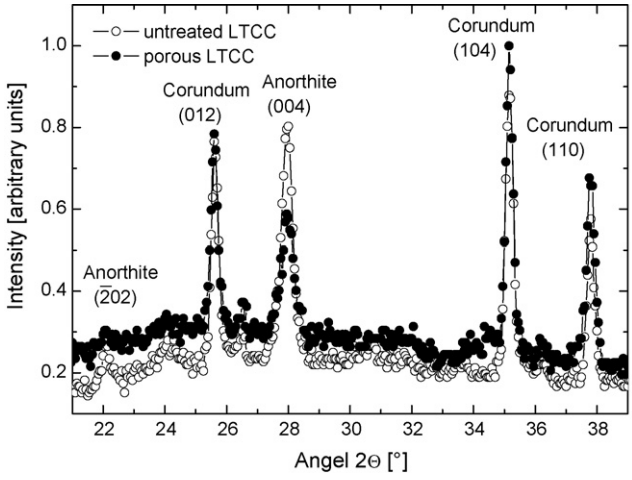

Fig. 8. µ-XRD spectra of LTCC before and upon exposure to phosphoric acid.

4. Conclusions

In this study, a novel process based on a wet chemical etchant is introduced to generate a tailored porosity in fired LTCC substrates (DP 951). Due to the use of a phosphoric acid which is well known for the patterning of aluminium thin films in MEMS or microelectronic industry a local porosification is feasible by using a photosensitive polyimide as mask material. The method is very simple to monitor, as important parameters, such as the bath temperature and the exposure time, strongly determine the degree and the depth of the porosification process. In addition, the LTCC fabrication process does not need to be changed, as porosification is generated in the fired state of commercially available tapes. Typically, this process step could be implemented in the flow chart of a device or module before final metallization. It could be demonstrated that at a bath temperature of 130 °C, the penetration depth has a maximum value of about 40 µm. To enable the penetration of the wet etchant into the LTCC body, this portion of the glass matrix enveloping the Al_2O_3 grains play an important role. In this area, anorthite crystallizes during liquid-phase sintering being preferentially etched compared to the alumina as well as to the residual glass matrix. With increasing exposure time, however, the dissolution of the Al_2O_3 grains becomes more pronounced, so that the originally gap-sized microstructure changes to a pore-sized geometry. Basically, the porosification process is reaction-limited at the beginning, while changing to a diffusion-controlled regime after an exposure time of about 5 h independent of bath temperature indicated by activation energies below 400 meV.

Acknowledgements

This work was performed within the RADARAUGE project (http://www.radarauge-project.com/) financially supported by the Federal Ministry of Education and Research (BMBF) under contract number 16SV2080. This support is gratefully acknowledged. Furthermore, the authors wish to express their thanks Dr. D. Schwanke and T. Haas being with the project partner Micro Systems Engineering GmbH for providing the LTCC substrates.

References

1. His, C. S., Hsieh, F. M. and Chen, H. P., Characteristics of thick film resistors embedded in low temperature co-fired ceramic (LTCC) substrates. *J. Eur. Ceram. Soc.*, 2007, **27**, 2779–2784.
2. Jantunen, H., Kangasvieri, T., Vähäkangas, J. and Leppävuori, S., Design aspects of microwave components with LTCC technique. *J. Eur. Ceram. Soc.*, 2003, **23**, 2541–2548.
3. Fonseca, M. A., English, J. M., Arx, M. V. and Allen, M. G., Wireless micromachined ceramic pressure sensor for high temperature applications. *J. Microelectromech. Syst.*, 2002, **11**, 337–443.
4. Heinonen, E., Juutu, J. and Jantunen, H., Characteristics of piezoelectric cantilevers embedded in LTCC. *J. Eur. Ceram. Soc.*, 2007, **27**, 4135–4138.
5. Gebhardt, S., Seffner, L., Schlenkrich, F. and Schönecker, A., PZT thick films for sensor and actuator applications. *J. Eur. Ceram. Soc.*, 2007, **27**, 4177–4180.
6. Birol, H., Maeder, T., Nadzeyka, I., Boers, M. and Ryser, P., Fabrication of a millinewton force sensor using low temperature co-fired ceramic (LTCC) technology. *Sens. Actuators A*, 2007, **134**, 63–70.
7. Schmid, U. and Seidel, H., Study on an injection quantity sensor. II. Evaluation of the sensing element. *J. Micromechatronics*, 2005, **3**, 33–50.
8. Rettig, F. and Moos, R., Ceramic meso hot-plates for gas sensors. *Sens. Actuators B*, 2004, **103**, 91–97.
9. Schmid, U., Seidel, H., Mueller, G. and Becker, Th., Theoretical considerations on the design of a miniaturised paramagnetic oxygen sensor. *Sens. Actuators B*, 2006, **116**, 213–220.
10. Hrovat, M., Belavic, D., Kita, J., Cilensek, J., Golonka, L. and Dziedzic, A., Thick-film temperature sensors on alumina and LTCC substrates. *J. Eur. Ceram. Soc.*, 2005, **25**, 3443–3450.
11. Golonka, L. J., Roguszczak, H., Zawada, T., Radojewski, J., Grabowska, I., Chudy, M., Dybko, A., Brzozka, Z. and Stadnik, D., LTCC based microfluidic system with optical detection. *Sens. Actuators B*, 2005, 111–112, 396–402.
12. Martínez-Cisneros, C. S., Ibáñez-García, N., Valdés, F. and Alonso, J., LTCC microflow analyzers with monolithic integration of thermal control. *Sens. Actuators A*, 2007, **138**, 63–70.
13. Gongora-Rubio, M. R., Espinoza-Vaaejobs, P., Sola-Laguna, L. and Santiago-Avilés, J. J., Overview of low temperature co-fired ceramics tape technology for meso-system technology (MsST). *Sens. Actuators A*, 2001, **89**, 222–241.
14. Dannheim, H., Schmid, U. and Roosen, A., Lifetime prediction for mechanically stressed low temperature co-fired ceramics. *J. Eur. Ceram. Soc.*, 2004, **24**, 2187–2192.
15. Dannheim, H., Roosen, A. and Schmid, U., Effect of metallization on the lifetime prediction of mechanically stressed low-temperature co-fired ceramics multilayers. *J. Am. Ceram. Soc.*, 2005, **88**, 2188–2194.
16. Ohnuki, Y., Ori, T., Yoshihare, K., Nonaka, Y., Senda, M. and Shibuya, H., Development of copper-polyimide thin film multilayer on LTCC substrate. In *Proceedings of International Microelectronics 1994 Conference (IMC)*, 1994, pp. 215–219.
17. Dernovsek, O., Preu, G., Wersing, W., Modes, C., Eberstein, M., Schiller, W., Güther, W. and Schulz, B., Glaskeramikmasse und Verwendung der Glaskeramikmasse. German Patent DE 10043194 A1, 2000.
18. Chen, G.-H., Effect of replacement of MgO by CaO on sintering, crystallization and properties of $MgO–Al_2O_3–SiO_2$ system glass–ceramics. *J. Mater. Sci.*, 2007, **72**, 7239–7244.
19. Jain, A., Rogojevic, S., Ponoth, S., Agarwal, N., Matthew, I., Gill, W. N., Persans, P., Tomozawa, M., Plawsky, J. L. and Simonyi, E., Porous silica materials as low-k dielectrics for electronic and optical Interconnects. *Thin Solid Films*, 2001, 398–399, 513–522.
20. Moh, K. H., Verbundstoffe auf Glasbasis und Glaskeramikbasis und Verfahren zu ihrer Herstellung. German Patent DE 4234349 C2, 1992.
21. Moh, H. K., Hoyle, C. D. and Boyer, C. E., Ceramic composite for electronic applications. US Patent US 5108958, 1990.
22. Kellerman, D., Improved micro-electronics devices and methods of manufacturing same. European Patent EP 0234896, 1987.
23. Morrison, W. H. Jr., Method for preparing ceramic tape compositions. US Patent US 4867935, 1989.
24. Schuler, K., Venot, Y. and Wiesback, W., Innovative material modulation for multilayer LTCC antenna design at 76.5 GHz in radar and communication applications. In *Proceedings of the 33rd European Microwave Conference, vol. 2*, 2003, pp. 707–710.
25. Lee, Y. C. and Park, C. S., Loss minimization of LTCC microstrip structure with air-cavities embedment in the dielectric. *Int. J. Electron. Commun.*, 2003, **6**, 429–432.
26. DuPont Photopolymer & Electronic Materials: 951 Low-Temperature Cofired Dielectric Tape, UK, 1998.
27. Deisinger, U., Stiegelschmitt, A., Roosen, A., Schwanke, D., Bechthold, F. and Schmaus, C., Charakterisierung und Schwindungsverhalten von LTCC-Grünfolien. *Plus*, 2001, **3**, 2–8 [in German].
28. Madou, M. J., *Fundamentals of Microfabrication* (*2nd ed.*). CRC Press LLC, Boca Raton, FL, 2002, pp. 206–220.
29. Jordan, G. and Rammensee, W., Dissolution rates and activation energy for dissolution of brucite (0 0 1): a new method based on the microtopography of crystal surfaces. *Geochim. Cosmochim. Acta*, 1996, **24**, 5055–5062.
30. Jean, J., Fang, Y., Dai, S. X. and Wilcox Sr., D. L., Effects of alumina on devitrification kinetics and mechanism of $K_2O–CaO–SrO–BaO–B_2O_3–SiO_2$ glass. *Jpn. J. Appl. Phys.*, 2003, **42**, 4438–4443.
31. Oelkers, E. H. and Schott, J., Experimental study of anorthite dissolution and the relative mechanism of feldspar hydrolysis. *Geochim. Cosmochim. Acta*, 1995, **59**, 5039–5053.
32. Lasagna, A. C., Chemical kinetics of water–rock interactions. *J. Geophys. Res.*, 1984, **B6**(89), 4009–4025.